Development 138, 995-1004 (2011) doi:10.1242/dev.061507

Neuronal subtype specification in the spinal cord of a protovertebrate

Alberto Stolfi and Michael Levine*

SUMMARY

The visceral ganglion (VG) comprises the basic motor pool of the swimming ascidian tadpole and has been proposed to be homologous to the spinal cord of vertebrates. Here, we use cis-regulatory modules, or enhancers, from transcription factor genes expressed in single VG neuronal precursors to label and identify morphologically distinct moto- and interneuron subtypes in the *Ciona intestinalis* tadpole larva. We also show that the transcription factor complement present in each differentiating neuron correlates with its unique morphology. Forced expression of putative interneuron markers *Dmbx* and *Vsx* results in ectopic interneuron-like cells at the expense of motoneurons. Furthermore, by perturbing upstream signaling events, we can change the transcription factor expression profile and subsequent identity of the different precursors. Perturbation of FGF signaling transforms the entire VG into *Vsx*$^{+}$/*Pitx*$^{+}$ putative cholinergic interneurons, while perturbation of Notch signaling results in duplication of *Dmbx*$^{+}$ decussating interneurons. These experiments demonstrate the connection between transcriptional regulation and the neuronal subtype diversity underlying swimming behavior in a simple chordate.

KEY WORDS: *Ciona*, Ascidian, Gene regulatory network, Spinal cord, Motoneurons

INTRODUCTION

Ascidians belong to the urochordates, or tunicates, which comprise the sister group to the vertebrates within the chordate phylum (Delsuc et al., 2006). Thus, ascidians (or sea squirts) are the extant invertebrates most closely related to vertebrates. The sea squirt *Ciona intestinalis* (to which we will now refer in this text as simply *Ciona*) has emerged as a model system for studying the regulation of chordate developmental processes (Satoh, 2003). Their small size, rapid development and deterministic cell lineages have long been appreciated by classical embryologists (Chabry, 1887; Conklin, 1905), while their compact genome and suitability to molecular perturbation and imaging have propelled them into the post-genome era (Dehal et al., 2002).

Although adult sea squirts feature numerous morphological adaptations to a life of sessile filter-feeding, their free-swimming tadpole larvae possess a typical chordate body plan. This includes a dorsally located central nervous system (CNS) derived from a neural plate that rolls up to form a hollow neural tube (Nicol and Meinertzhagen, 1988). The *Ciona* larval CNS comprises ~335 cells, of which roughly one third are neurons (Nicol and Meinertzhagen, 1991). They arise through evolutionarily conserved, invariant cell lineages that have been described in detail (Cole and Meinertzhagen, 2004). The CNS is divided along the anterior-posterior axis into distinct anatomical regions. At its most anterior lies a sensory vesicle containing melanized pigment cells and associated sensory cells that sense light and gravity (Dilly, 1964; Dilly, 1962; Sato and Yamamoto, 2001). The majority of neurons of the CNS are located in a tight cluster associated with this sensory vesicle. Immediately posterior to the sensory vesicle and associated neurons lies the 'neck', which comprises a few quiescent precursors in larvae (Nicol and Meinertzhagen, 1991). After metamorphosis, these precursors differentiate into the branchial basket motoneurons of the adult that are thought to be homologous to the cranial motoneurons of the vertebrate hindbrain (Dufour et al., 2006).

Further posterior is a 'visceral ganglion' (VG), which consists of cholinergic neurons innervating the longitudinal muscle bands on either side of the tail. These muscles contract in left/right alternation to produce the vigorous swimming behavior that aids in the dispersal of the larvae (Brown et al., 2005; Horie et al., 2010; Ohmori and Sasaki, 1977; Takamura et al., 2002). These neurons are thought to receive inputs from the sensory vesicle, as well as from the peripheral nervous system (Horie et al., 2008a; Takamura, 1998). It has been shown that swimming behavior is modulated by light and gravity (Horie et al., 2008b; Jiang et al., 2005; Tsuda et al., 2003), and that the response of the larvae to these stimuli can change over time (Kajiwara and Yoshida, 1985). Thus, the CNS of the ascidian larva can be seen as a central pattern generator for swimming, modulated by photo- and geotropic sensory systems (Goulding, 2009).

Gene expression studies suggest that many of the molecular mechanisms underlying the patterning of the ascidian larval CNS are shared with vertebrates (Meinertzhagen et al., 2004; Meinertzhagen and Okamura, 2001). Some of these conserved mechanisms, such as dorsoventral patterning involving *Pax3/7* (Wada et al., 1997), anteroposterior patterning by retinoic acid (Nagatomo and Fujiwara, 2003) and organizer activity of FGF8/17/18 (Imai et al., 2009), have so far been observed only in chordates. As such, *Ciona* has the potential to serve as a model system for studying chordate-specific gene regulatory networks underlying the development of the CNS.

Recently, preliminary gene regulatory networks have been described at single-cell resolution for each cell in the vegetally derived neural plate and neural tube in the embryo up to the tailbud stage (Imai et al., 2006; Imai et al., 2009). In other studies, the morphological diversity of CNS neurons in swimming larvae has

Center for Integrative Genomics, Division of Genetics, Genomics and Development, Department of Molecular and Cell Biology, University of California, Berkeley, CA 94720, USA.

*Author for correspondence (mlevine@berkeley.edu)

Accepted 7 December 2010

been described using fluorescence microscopy (Imai and Meinertzhagen, 2007; Okada et al., 2001; Takamura et al., 2010; Yoshida et al., 2004). However, because pan-neural or neurotransmitter-related fusion genes were used to visualize the neurons, as opposed to individually labeling them, the identities and lineages of these cells remain uncertain. Thus, there is a gap in information between the cell lineages and gene regulatory networks in the embryo, and the final morphology of the differentiated neurons of the tadpole.

In this study, we use fusion genes containing *cis*-regulatory elements ('enhancers') from several regulatory genes to label unique pairs of cells in the developing VG and visualize them in their final differentiated state in swimming larvae. Included in this analysis are enhancers from *Ciona* orthlogs of transcription factors known to play a role in neuronal specification and differentiation in the spinal cord of vertebrates, such as *Dmbx1, Vsx2/Chx10, Islet1*, *Nkx6*, *Pitx2* and *Onecut/Hnf6*. These fusion genes (hereafter termed 'reporter constructs') revealed morphological traits that are specific to single pairs of VG neurons. Furthermore, we present evidence that the morphology of distinct VG neuronal subtypes is regulated by these transcription factors, and that the FGF and Notch signaling pathways establish the unique expression profiles of each differentiating VG neuron.

MATERIALS AND METHODS

Molecular cloning

Cis-regulatory regions of *Dmbx*, *Vsx*, *Nk6*, *Coe* and *Onecut* were obtained by PCR off genomic DNA template isolated from California *C. intestinalis* adults using the following primers (all sequences indicated as 5′ to 3′, from left to right): *Dmbx* –3.5 kb F, CACTCATCTGCCTACATTAGC; *Dmbx* –1 start R, TATGACGTATAGAAGCAGTGG; *Vsx* exons/introns F, GGTTCAAATCGGATGAAAC; *Vsx* exons/introns R, ATTCTTC-CTTCGAGCATTGAC; *Nk6* intron1 F, TCGCAAAAATGCGC-CGACAAG; *Nk6* intron2 R, TGGAACCAAACCTACCAATGG; *Coe* –2.6 kb F, GTCCATTATTTGTCTGCAGGG; *Coe* +8 start mutATG R, TCCCGCGATTGTTGCCATTTG; *Onecut* –4.2 kb F: TCGTTCGTCGT-CTAACAGACG; *Onecut* +105 R, CATAGTGATGAAGTCCGTTGC.

Restriction enzyme sites were designed to the 5′ end of these oligonucleotides in order to clone the fragments into reporter expression plasmids. *Dmbx*, *Coe* and *Onecut* regulatory regions contained their respective endogenous basal promoters. In the case of *Dmbx,* the reverse primer was just 5′ of the putative start codon, while for *Coe*, the start codon was mutated. *Vsx* and *Nk6* exonic/intronic fragments were cloned upstream of the basal promoter from the friend of GATA gene (bpFOG) (Rothbächer et al., 2007), fused in frame to the reporter gene. For double-electroporation with *Dmbx* reporter construct, a smaller fragment containing DNA –3.5 kb to –2.1 kb upstream of the *Dmbx* transcription start site was amplified using *Dmbx* –3.5 kb F and *Dmbx* –2.1 kb R (AGTACTATGACGTTACAATCC), and cloned upstream of bpFOG in order to minimize reporter construct crosstalk. A smaller 279 bp fragment within the 3rd intron of *Vsx* was found to be sufficient to recapitulate *Vsx* expression, and was sometimes used in place of the larger fragment. This smaller piece was amplified using *Vsx* intron3 F (GTTTGTCATTTTCGTTCCTTGG) and *Vsx* intron 3 R (AGAAGAAGTACAGGTCTCACC), and cloned upstream of bpFOG. Plasmids were constructed using pCESA backbone (Corbo et al., 1997). Previously published drivers used in this study include *Fgf8/17/18* (Imai et al., 2009), *Islet* (Stolfi et al., 2010) and *Pitx* proximal fragment (Christiaen et al., 2005). To minimize promoter crosstalk, a smaller ~3.4 kb fragment including the 'P3' and 'P1' elements from the *Pitx* proximal regulatory regions was amplified using *Pitx* P3 F (CTTAAGTCACGCGAAATGCC) and *Pitx* P1 R (GTGTCGTCTAACTTGTTCTC) and cloned upstream of bpFOG.

The reporter genes used were *lacZ* with a nuclear localization signal or *unc-76*-tagged fluorescent proteins that label axons more efficiently than untagged versions (Dynes and Ngai, 1998). In a few instances, F-actin-binding GFP::Moesin fusion was used (Edwards et al., 1997).

Dmbx, Vsx, Nk6 and *Islet* protein-coding cDNA sequences were amplified by RT-PCR. First-strand cDNA synthesis was performed off mixed-stage embryo whole mRNA preparations using oligo-dT primer. For PCR, the following primers were used (left to right=5′ to 3′): *Dmbx* cDNA N F, ATGAATTATTATGACGCAATTCGTGC; *Dmbx* cDNA C R, CGATT-ACATCATCATTTCTTGGATTG; *Vsx* cDNA N F, ATGATT-ACGTCACTCAAAAGAAG; *Vsx* cDNA C R, TCATTCTTC-CTTCGAGCATTG; *Nk6* cDNA N F, ATGTCCATGGAAGAATCTGG; *Nk6* cDNA C R, AACTTGTACAAAGCAGATGTC; *Islet* cDNA N F, ATGAACGAATCATTCGCCATTTTC; *Islet* cDNA C R, TTAGCTACACGCCGGTACAGTTG.

Dmbx, Nk6 and *Islet* primers were designed based on available mRNA, EST and genomic sequence data. *Vsx* gene prediction models were incomplete, and thus the 5′ and 3′ ends were determined by SMART RACE cDNA amplification kit (Clontech), using gene-specific primers Vsx GSP1 (TCTGCCATAACGCTACTCTTGCCCCAAC) and Vsx GSP2 (TCTTGCTCATTACCCGGATGCAGAAACG) for 5′-RACE and 3′-RACE, respectively. This revealed a 1563 bp sequence coding for an open reading frame of 521 amino acids. Outside the highly conserved homeodomain, this ORF showed stretches that were similar to the *Ciona savigny* ortholog of *Vsx*, but not to vertebrate or non-chordate orthologs.

Su(H)DBM (Hudson and Yasuo, 2006) and *dnFgfr* (Davidson et al., 2006) have been previously described and were cloned downstream of the *Fgf8/17/18* driver.

In situ hybridization probes

Dmbx and *Vsx* probe template was prepared by cloning the coding sequence of either into pBSKM, the plasmid backbone of *Ciona intestinalis* gene collection library clones, linearized with *Kpn*I and *Not*I. A 1 kb fragment from the coding sequence of *Nk6* was amplified with Nk6 cDNA N F primer and Nk6 1kb C R primer (ATCACTTCCTTCATGCTCGC) and cloned in the same backbone with *Kpn*I and *Not*I. Antisense ribonucleotide probe was synthesized in vitro using T7 polymerase (Roche), cleaned up with RNAse-free DNAse I (Roche) and purified using RNeasy Mini Kit columns (Qiagen).

Embryo handling, manipulation and analysis

Islet (ciad008c12) template was retrieved from said gene collection. All template plasmids were linearized with *Not*I or *Spe*I and digoxigenin-UTP-labeled probe made by in vitro transcription with T7 RNA polymerase (Roche). Adult *Ciona intestinalis* were obtained from Pillar Point marina (Half Moon Bay, CA) or purchased from M-Rep (San Diego, CA). Fertilization, dechorionation, electroporation, fixation, counterstaining and mounting of embryos was carried out as established (Christiaen et al., 2009). Each electroporation used 50-100 μg of plasmid. Histone2B-fluorescent protein fusions are very stable and bright, and thus only 5-10 μg of these plasmids was needed per electroporation. The technique of 'consecutive electroporation' consisted of electroporating embryos with one plasmid mix, rinsing in sea water by transferring to new dishes and gentle swirling, then electroporation with a second plasmid mix. Fluorescent in situ hybridization coupled to β-galactosidase immunodetection was performed using a TSA-plus fluorescein tyramide signal amplification kit (Perkin-Elmer) and monoclonal mouse anti-β-galactosidase antibody (Promega #Z378A) as previously described (Beh et al., 2007). Embryos were imaged using Nikon or Zeiss upright microscopes. Staging was estimated in hours after fertilization at 16°C, and confirmed by counting A9.30 lineage cells according to the mitotic history and staging nomenclature established for the neural tube (Cole and Meinertzhagen, 2001; Cole and Meinertzhagen, 2004).

RESULTS

Detailed descriptions of the mitotic history of the neural tube of *Ciona* have identified the precise lineages of the five pairs of cholinergic neurons comprising the VG (Cole and Meinertzhagen, 2004). Hereafter, we will refer to them as single cells on either side of the embryo: the four anteriormost neurons are descended from the A9.30 blastomere (in order, from anterior to posterior: A12.239,

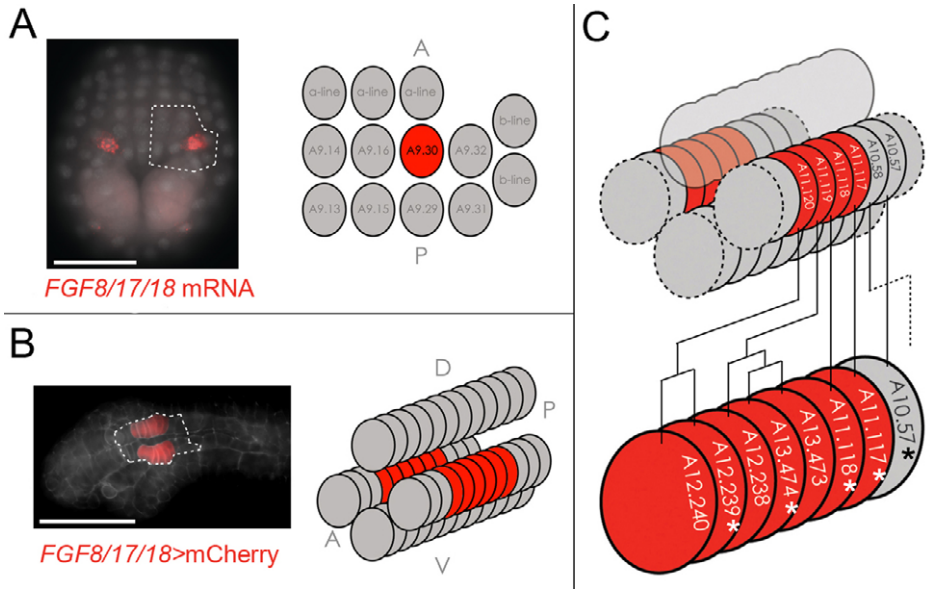

Fig. 1. Cell lineages of the visceral ganglion. (**A**) Dorsal view of a late gastrula embryo with A9.30 blastomeres labeled by in situ hybridization for *Fgf8/18/19* mRNA in red. Cell nuclei are counterstained by Hoechst stain. Outlined are the cells represented in the diagram on the right, representing the right half of the bilaterally symmetric posterior neural plate. (**B**) Lateral view of a stage E65-E70 tailbud embryo [~15 hours post-fertilization (hpf) at 16°C], with descendants of A9.30 labeled by mCherry driven by the *Fgf8/17/18* enhancer in red. Cell membranes are counterstained with phallicidin:BODIPY-FL. Outlined are the cells represented in the diagram on the right, representing the posterior neural tube, comprising four rows of cells and derived from the posterior neural plate depicted in A. The dorsal row of cells is slightly lifted to reveal descendants of both A9.30 blastomeres (red) on either side of the embryo. (**C**) Top: neural tube at E60 (~12 hpf), with A9.30 and A9.29 descendants labeled according to the established nomenclature (from anterior to posterior: A11.120, A11.119, A11.118, A11.117, A10.58, A10.59). Dorsal row is rendered translucent for visualization of right lateral row; dashed outlines represent more anterior or posterior cells of the neural tube that have been omitted. A9.30 descendants are highlighted in red, representing labeling by the *Fgf8/17/18* reporter construct (see text for details). Bottom: A9.30 lineage plus A10.57 on one side of the embryo at E75-E80 (~16 hpf). Lines between top and bottom diagrams denote invariant cell lineages. Dotted line represents posterior displacement of A10.58 by directed migration of A10.57. Putative motoneurons are denoted by asterisks. A, anterior; P, posterior; D, dorsal; V, ventral. Scale bars: ~50 μm.

A13.474, A11.118, A11.117), while the posterior-most 5th neuron (A10.57) is the posterior daughter cell of the A9.29 blastomere (summarized in Fig. 1C). We have previously shown that electroporation of 4.8 kb of genomic DNA located immediately upstream of the *Fgf8/17/18* transcription start site fused to a reporter gene preferentially labels cells descended from the A9.30 blastomere, as *Fgf8/17/18* is strongly expressed in A9.30 at the late gastrula stage (Fig. 1A,B) (Imai et al., 2009).

Cell-specific reporter gene expression reveals neuronal subtypes in the VG

By coupling fluorescent in situ hybridization to immunofluorescence-based detection of β-galactosidase driven by the *Fgf8/17/18* enhancer, we visualized, with single-cell resolution, the expression patterns of three homeodomain-containing transcription factors (TFs): *Dmbx, Vsx* (also known *Chx10*) and *Islet* (Fig. 2A-C). These were described in previous studies as being exclusively expressed in a single pair of cells in the developing VG. Double in situ hybridization/antibody stains confirmed previous reports that, at the tailbud stage, *Dmbx* is expressed only in the A12.239 pair (Ikuta and Saiga, 2007; Takahashi and Holland, 2004), and Islet is expressed only in the A10.57 pair, in addition to being expressed in other tissues such as notochord, palps, pharyngeal mesoderm and bipolar tail neurons (Giuliano et al., 1998; Stolfi et al., 2010). In the distantly related ascidian *Halocynthia roretzi*, *Islet* has been shown to be transiently expressed in the A9.30 lineage, but maintained late only in A10.57 (Katsuyama et al., 2005). Similarly, we confirmed that *Islet* expression in the VG is eventually restricted to A10.57 (Imai et al., 2009). *Vsx* was found to be expressed by two pairs of neurons, initially being expressed in A11.117, and later in A13.474. This difference in the onset of *Vsx* expression is consistent with the difference in specification of these two pairs of neurons: A11.117 ceases mitotic activity at a time when A13.474 has not yet been born.

We next searched for enhancers in or surrounding these three genes that would be sufficient to recapitulate their cell-specific patterns. A fusion of 3.5 kb of Dmbx upstream DNA with *unc-76*-tagged enhanced green fluorescent protein (GFP) recapitulated strong expression in A12.239, with slight expression in its sister cell, A12.240 (Fig. 2D). Similarly, a DNA sequence spanning the entire *Vsx* transcribed region recapitulated expression in A11.117 and A13.474 (Fig. 2E, Fig. 3B), suggesting the presence of an intronic enhancer. Finally, we have previously described an upstream enhancer of *Islet* that drives reporter gene expression in A10.57 (*'Islet>GFP'*) (Stolfi et al., 2010), which we have also used in this study (Fig. 2F).

Dmbx in A12.239

When embryos electroporated with such reporter constructs were allowed to develop until hatching, we were able to visualize individual terminally differentiated neurons. A12.239, as revealed by *Dmbx>mCherry*, shows a thin axon projecting down the tail. However, it does not form the conspicuous, frondose endplates at the base of the tail revealed by electroporation of pan-neural reporter constructs (Imai and Meinertzhagen, 2007). Furthermore,

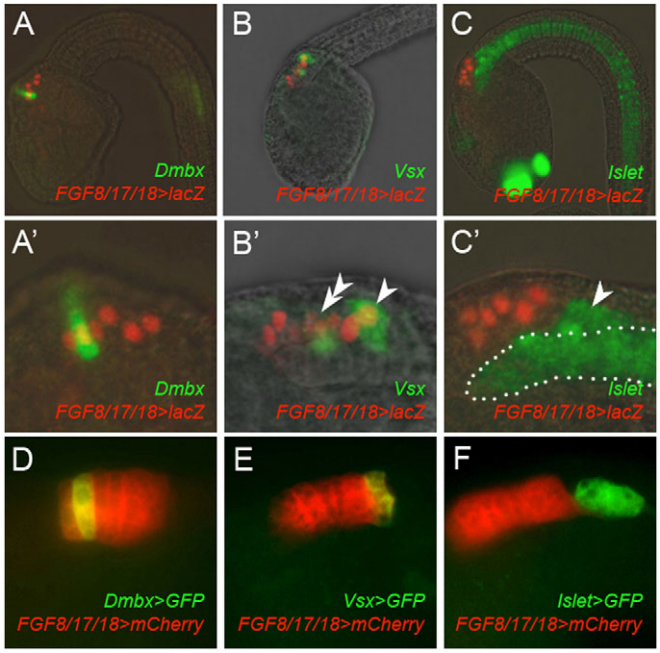

Fig. 2. *Dmbx, Vsx* and *Islet* expression in the developing VG of tailbud embryos. (**A**) In situ hybridization of *Dmbx* in green, showing expression in only A12.239. (**A′**) Higher magnification of A. (**B**,**B′**) In situ hybridization of *Vsx* in green, showing expression in A11.117 and A13.474 (arrowhead and double arrowhead in B′, respectively. (**C**,**C′**) In situ hybridization of *Islet* in green, showing expression in A10.57 (arrowhead in C′). Strong signal also seen in other tissues, including notochord (broken outline in C′). All embryos counterstained by fluorescent antibody stain for β-gal (red nuclei), denoting A9.30 lineage labeled by electroporation with *Fgf8/17/18>lacZ*. (**D-F**) Embryos co-electroporated with *Fgf8/17/18>mCherry* (red) and *Dmbx* (D), *Vsx* (E) or *Islet>GFP* (green) (F). Colocalization of GFP and mCherry is indicated in yellow and corresponds to A12.239 in D and A11.117 in E. *Vsx>GFP* is not seen in A13.474 in E, as this cell has not yet been born. As expected, colocalization is not seen in F, as A10.57 is not a part of the A9.30 lineage. Embryos in A-E are stage E65-70 (~15 hpf); embryo in F is stage E75-E80 (~16 hpf). All are lateral views.

the A12.239 pair project contralaterally, each axon associating with the axon bundle on the opposite side of the embryo (Fig. 3A). This is more clearly demonstrated by left/right mosaic expression, which can be achieved by consecutive electroporation of different reporter plasmid mixtures (Fig. 3D).

Thus, A12.239 is the pair of contralaterally projecting VG neurons that were recently identified and likened to Mauthner neurons of rhombomere 4 of the fish and amphibian hindbrain (Takamura et al., 2010). Mauthner neurons are important for the escape response in which the animal rapidly turns its body away from an auditory stimulus (Eaton et al., 2001). Mauthner neuron axons cross the midline and synapse onto spinal cord motoneurons on the other side. The contralateral projection of A12.239 and their lack of endplates suggests they could serve to modulate motoneurons in a similar way, perhaps modulating the asymmetric ‘tail flicking’ behavior of the tadpole (Mackie and Bone, 1976). The comparison to Mauthner cells could distinguish A12.239 from the rest of the VG. If this homology holds up, one could assign these neurons a higher-order status in the motor network, a rudiment of the posterior hindbrain of vertebrates.

Despite a contralateral projection that could in theory help establish left/right coordination of muscle contraction during swimming, A12.239 expresses cholinergic markers and is not believed to be an inhibitory interneuron (Ikuta and Saiga, 2007). GABAergic interneurons that arise from a different lineage are situated at the base of the tail and contact the motoneuron axon bundles in a contralateral manner (Brown et al., 2005; Horie et al., 2010). These are more likely to serve as inhibitory interneurons for modulating oscillatory left/right motoneuron firing.

Vsx in A13.474 and A11.117, Pitx in only A11.117

Neurons A13.474 and A11.117, as revealed by *Vsx>GFP* or *mCherry* (Fig. 3B), have thin axons and do not form conspicuous endplates, but do not appear to project contralaterally. Their axons never cross the midline as they project down the tail. The two pairs are distinguished by cell body size. A13.474 has a smaller cell body than that of A11.117 and the other neurons (Fig. 3B,E). Furthermore, *Vsx>GFP* revealed neurites emanating from the soma of A11.117 but not of A13.474, possibly representing dendrites (Fig. 3E). These dendrites were not seen on any of the other neurons.

The two *Vsx*-expressing pairs of neurons were separately labeled by co-electroporation with *Pitx* reporter constructs. A proximal genomic DNA fragment that drives the expression of the homeodomain TF *Pitx* in the visceral ganglion has been previously described (Christiaen et al., 2005). Electroporation of embryos with *Pitx>mCherry* specifically labeled A11.117 but not A13.474 (Fig. 3F,G). Co-labeling with *Vsx>GFP* and *Pitx>mCherry* also shows that A13.474 lacks the putative dendrites that are specific to A11.117 (Fig. 3G,H). *Pitx* reporter gene expression was not seen prior to hatching (data not shown), suggesting *Pitx* is activated in A11.117 downstream of *Vsx*.

Recently, *Pitx2* was identified as a novel marker of cholinergic spinal interneurons in mouse (Enjin et al., 2010). A11.117 is also cholinergic and its lack of endplates further suggests a cholinergic interneuron identity. By contrast, *Vsx* orthologs are more broadly associated with interneurons arising in different nervous tissues and expressing different neurotransmitters (Kimura et al., 2006; Svendsen and McGhee, 1995). Therefore, the combination of *Vsx* and *Pitx* could be important for the specification of a cholinergic spinal interneuron identity.

Islet in A10.57

A10.57, as revealed by *Islet>mCherry* or *GFP* and in accordance with previous studies, displays a cell body more elongated along its anterior-posterior axis than the other VG neurons (Imai and Meinertzhagen, 2007; Okada et al., 2002), but does not form prominent endplates (Fig. 3C,D). Putative motor endplates labeled by the *Islet* reporter were consistently smaller than the frondose endplates revealed by pan-neural reporter constructs (see Fig. S1 in the supplementary material).

Nk6 in A11.118

The preceding reporter constructs revealed the morphology of four out of five pairs of neurons in the VG, yet the frondose endplates still escaped cell-specific labeling. A fourth reporter construct, composed of the transcribed region of the *Nk6* gene fused to GFP, stained frondose endplates in ~50% of transfected embryos (Fig. 4A; see Fig. S2 in the supplementary material). This indicated the presence of an intronic enhancer. In half these cases, the staining was associated mainly with one cell body (see Fig. S2 in the supplementary material). Upon co-electroporation of

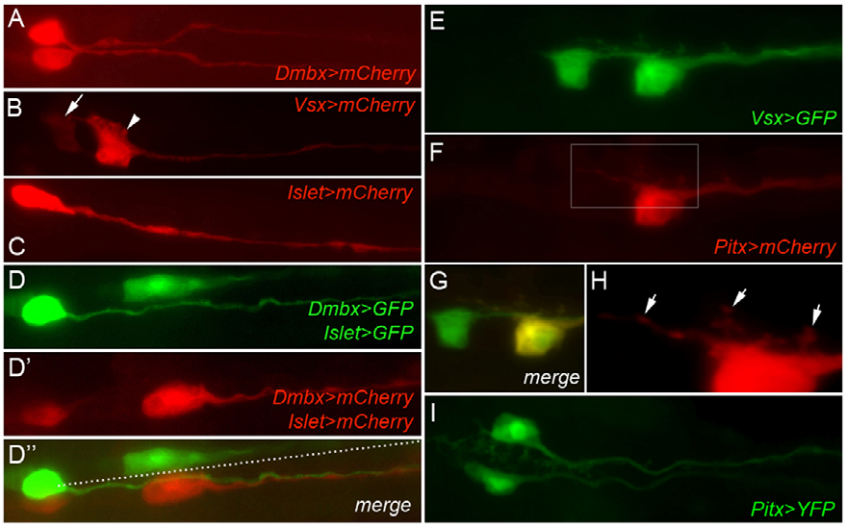

Fig. 3. Reporter constructs label individual differentiated VG neurons in the swimming tadpole. (**A**) Dorsal view of A12.239 pair labeled with *Dmbx>mCherry.* (**B**) Lateral view of A13.474 (arrow) and A11.117 (arrowhead) on left side labeled with *Vsx>mCherry* (red). (**C**) Lateral view of A10.57 labeled with *Islet>mCherry.* (**D-D″**) Successive electroporation results in a rare tadpole with mutually exclusive left-right mosaic uptake of *Dmbx>GFP* + *Islet>GFP* and *Dmbx>mCherry* + *Islet>mCherry* plasmid combinations. (D) Cell bodies of A12.239 and A10.57 on the right side of the embryo labeled with GFP. (D′) Cell bodies of A12.239 and A10.57 on the left side of the embryo labeled with mCherry. When red and green channels are merged (D″), the axon from GFP-labeled A12.239 on the right traverses the midline (dotted line) to associate with the mCherry-labeled axon of A10.57 on the left side, demonstrating the contralateral projections of the A12.239 pair. (**E**) Embryos electroporated with *Vsx>GFP,* which labels A13.474 and A11.117 pairs. (**F**) *Pitx>mCherry*, by contrast, labels only A11.117. (**G**) Merged image of E and F. A13.474 does not appear to have dendrites. (**H**) Magnified view of inset in F, showing putative dendrites belonging to A11.117 (arrows). (**I**) Dorsal view of an embryo electroporated with *Pitx>YFP,* showing labeling of both left and right cells in the A11.117 pair. The dendrites are oriented towards the midline, and the axons do not project contralaterally.

Nk6>mCherry and *Vsx>GFP*, this cell body was shown to be situated between A13.474 and A11.117 (Fig. 4D) and probably corresponds to A11.118.

This staining by the *Nk6* reporter construct was unexpected, because, at the tailbud stage, Nk6 is expressed throughout the developing VG. This preferential labeling of A11.118 might be due to maintenance of *Nk6* in this cell later in development. In situ hybridization of *Nk6* coupled to immunodetection of β-galactosidase in embryos electroporated with *Vsx>lacZ* is consistent with the preferential labeling of A11.118 by *Nk6>GFP* (Fig. 4B). Co-electroporation of *Nk6>GFP* and *Dmbx>mCherry* or *Islet>mCherry* further supported our conclusion that this late *Nk6*+ cell is A11.118 and that it is the only motoneuron to form the frondose endplates contacting the lateral surfaces of the anterior tail muscle cells (Fig. 4C,E). In fact, co-electroporation with *Islet>mCherry* suggested that A10.57 might modulate A11.118

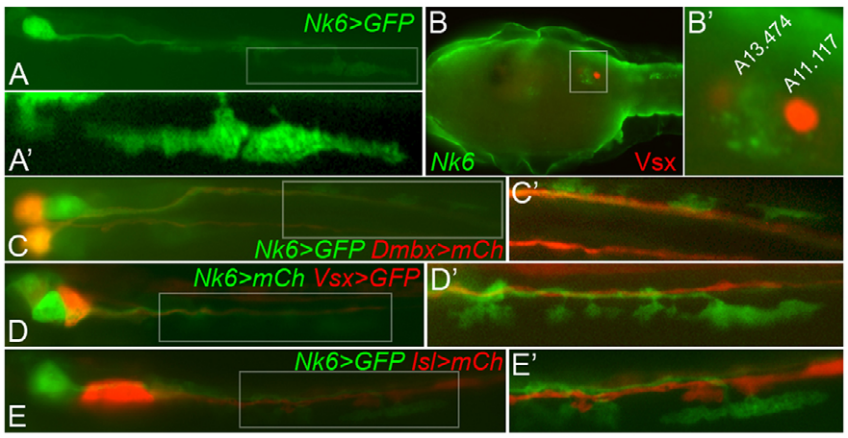

Fig. 4. Nk6 reporter reveals frondose motor endplates of A11.118. (**A**) *Nk6>GFP* reporter construct labels frondose motor endplates in 50% of electroporated embryos (see text for details). (**A′**) Magnified view of boxed area in A. (**B**) Late Nk6 expression (green) seen in stage E90 embryos in between cells A13.474 and A11.117 as revealed by antibody staining for β-gal in embryos electroporated with *Vsx>lacZ.* (**B′**) Magnified view of boxed area in B. (**C**) Larva electroporated with *Nk6>GFP* (green) and *Dmbx>mCherry* (red). (**D**) Larva electroporated with *Nk6>mCherry* (green) and *Vsx>GFP* (red). False-color scheme is inverted for consistency in the presentation of the data. (**E**) Larva electroporated with *Nk6>GFP* (green) and *Islet>mCherry* (red). (**C′-E′**) Magnified or different focal planes of areas boxed in C-E to highlight frondose endplates always labeled by the *Nk6* reporter construct, but not by *Dmbx*, *Vsx* or *Islet* reporters.

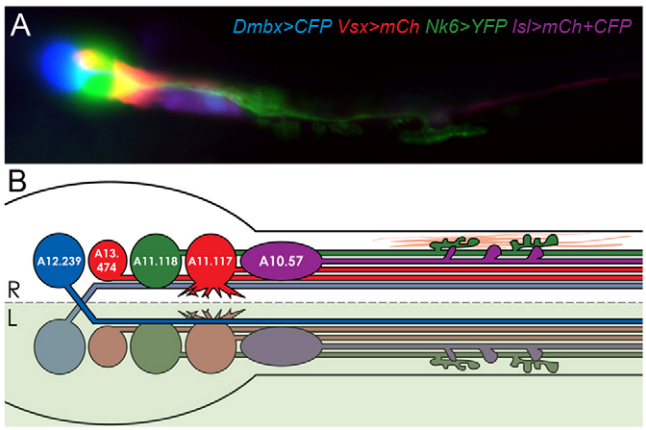

Fig. 5. The *Ciona* visceral ganglion 'brainbow'. (**A**) Merged image of an imaged larva electroporated with a combination of the following plasmids: *Dmbx>CFP* (blue), *Vsx>mCherry* (red), *Nk6>YFP* (green), and *Islet>mCherry* and *Islet>CFP* (purple). Thus, five MNs are simultaneously visualized and distinguishable from one another. Green channel was imaged on a different focal plane than blue or red, to visualize *Nk6>YFP*-labeled endplates. Yellow color only indicates overlap of cell bodies, not colocalization. (**B**) The neurons depicted in A and their unique morphological traits, such as contralateral projection of A12.239 pair, smaller cell body of A13.474, frondose endplates of A11.118, dendrites on A11.117, and elongated cell body and smaller endplates of A10.57. Pale-green shading indicates left side of the larva. Pink fibers represent tail muscle.

presynaptically, by what appears to be contacts onto the frondose endplates themselves (Fig. 4E; see Fig. S1B in the supplementary material).

None of the neurons exhibit an axon trajectory along the middle or ventral bands of the tail muscle, as was observed in the larvae of *Halocynthia* (Okada et al., 2002) and another ascidian species, *Dendrodoa grossularia* (Mackie and Bone, 1976). This difference in innervation could be due to the difference in size between the larger *Halocynthia* and *Dendrodoa* larvae relative to *Ciona*. In *Halocynthia*, the middle band-innervating neuron is termed 'Moto-b', but it is not known whether 'Moto-b' corresponds to A11.117 or A11.118. It is conceivable that the frondose endplates of A11.118 in *Ciona* could represent the vestiges of the more ventral axon trajectories seen in *Halocynthia* and *Dendrodoa*.

Ectopic Dmbx or Vsx expression abolishes A11.118-specific motor endplates

Our observations on the morphological diversity of the visceral ganglion (summarized in Fig. 5) raised the possibility that the unique TF expression profile of each VG precursor might be functionally related to their particular identity. To investigate the potential role of these TFs in regulating morphology in the VG, we misexpressed Dmbx, Vsx, Islet and Nk6 in all differentiating VG neurons using regulatory DNA from the *Coe* gene. *Coe* (*Collier/Olf/Ebf*) transcription factors are involved in myriad cell fate decisions in metazoans, particularly in neurogenesis (Dubois and Vincent, 2001). A 2.6 kb genomic DNA segment located upstream of the *Coe* gene directs expression in all of the differentiating VG neural precursors (see Fig. S3 in the supplementary material).

The visualization of individual neurons was sometimes compromised upon misexpression of certain TFs (see Fig. S4 in the supplementary material). For example, cross-repressive interactions between Dmbx, Vsx, and Islet were revealed by *in situ* hybridization assays (Fig. 6A-C). Dmbx and Vsx strongly repress each other (Fig. 6A,B), while Dmbx and Islet have seemingly little effect on each other's expression (Fig. 6A,C). Vsx can actually induce ectopic *Islet* expression (Fig. 6C), while Islet can repress *Vsx* in A13.474, but not in A11.117 (Fig. 6B), hinting at a more complicated interaction between these two genes.

This modulation in reporter construct expression did not allow us to fully characterize the morphology of individual cells under these conditions. There were no obvious morphological defects under conditions without cross-repression (e.g. *Islet>Dmbx*, data not shown). Nonetheless, using *Fgf8/17/18>GFP* to label all neurons in the A9.30 lineage we were able to visualize their axons in swimming larvae. Using this reporter, we observed multiple axons and axon growth cones originating from the VG in larvae electroporated with *Coe>Dmbx* (Fig. 6A,D,H; see Fig. S5A in the supplementary material). These axons were all thin and did not form frondose endplates like those seen in control larvae electroporated with *Coe>lacZ* (Fig. 6H; see Fig. S5B in the supplementary material). Electroporation of *Coe>Vsx* also mimicked this phenotype (Fig. 6E,H), suggesting that exclusion of Dmbx and/or Vsx from A11.118 might be important for its specification. By contrast, electroporation of *Coe>Nk6* or *Coe>Islet* did not have a visible effect on motor endplate formation (Fig. 6F-H). This observation is not surprising as *Nk6* and *Islet* are transiently expressed in A11.118 in wild-type larvae.

Conversion of visceral ganglion precursors into ectopic A11.117-like neurons

The preceding results are consistent with the idea that a transcription factor code is required for the specification of morphologically distinct neuron subtypes. However, the cross-repressive interactions not only interfered with our ability to distinguish individual cell bodies and axons, they also meant that certain driver>transgene combinations (e.g. *Vsx>Dmbx*) could not work owing to strong auto-repression.

In an effort to circumvent this problem, we manipulated candidate upstream cell signaling events. The goal was to change the identity of some cells without losing expression of the reporter constructs used for visualizing morphology and axon trajectories.

FGF signaling has been shown to be a major mechanism of cell fate specification in the *Ciona* neurogenic ectoderm (Bertrand et al., 2003; Hudson et al., 2007). We asked whether FGF signaling is involved in specifying the identity of the various neuron subtypes in the VG. The *Fgf8/17/18* enhancer was used to drive expression of a truncated, dominant-negative FGF receptor [dnFGFR (Davidson et al., 2006)] in A9.30. Lineage-specific perturbation of signaling downstream of FGFR resulted in ectopic A11.117-like cells. In 90% (n=90) of electroporated embryos, all A9.30 descendants express *Vsx>GFP* (Fig. 7B). By contrast, ectopic *Vsx>GFP* expression (in cells other than A11.117 and A13.474) is seen in only 11% (n=75) of control embryos co-electroporated with *Fgf8/17/18>lacZ*. These ectopic A11.117-like cells all project axons down the tail but do not form endplates (Fig. 7C). These neurons also express *Pitx>YFP*, albeit more weakly, indicating perhaps some later requirement for FGF signaling in *Pitx* activation or an inhibitory effect of excess Vsx (see Fig. S6D in the supplementary material). *Dmbx>GFP* reporter gene expression was completely abolished (see Fig. S6C in the supplementary material).

These results are consistent with a conversion of the entire lineage to an A11.117-like identity (summarized in Fig. 7H). Ectopic dendrites were not seen. This could be due to non-cell

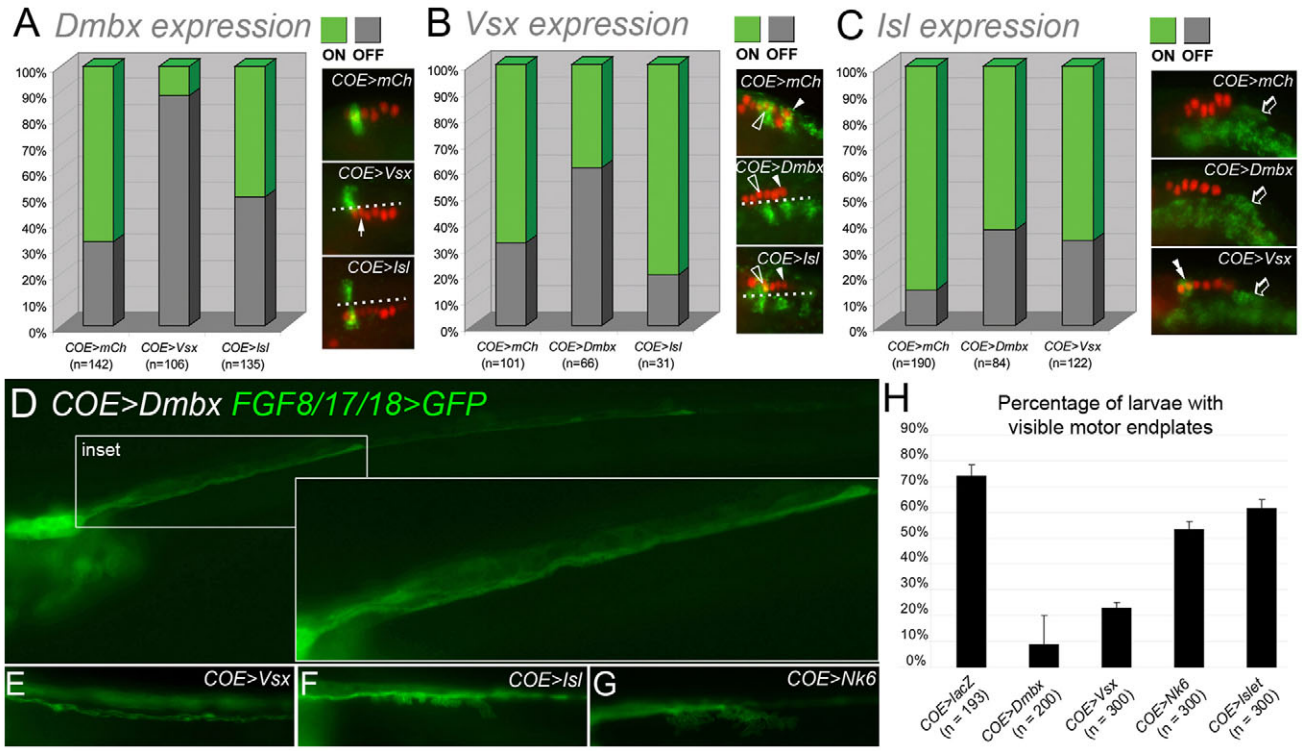

Fig. 6. Effects of ectopic expression of Dmbx, Vsx, Isl and Nk6. (**A**) Percent of electroporated embryos showing *Dmbx* expression upon electroporation with *Coe>mCherry* (control condition), *Coe>Vsx* or *Coe>Islet*. Only FGF8/17/18>lacZ+ embryo hemispheres (left/right) were assayed for colocalization with *Dmbx* transcript (by immunofluorescence staining for β-gal coupled to fluorescent in situ hybridization). Green shading indicates the fraction of β-gal+ embryo hemispheres showing *Dmbx* expression. Grey shading indicates the fraction of β-gal+ hemispheres that do not show expression of *Dmbx*. Paucity of colocalization relative to control indicates that the transcription factor being overexpressed probably represses *Dmbx*. Panels to the right of the graph are representative embryos from each condition, showing A9.30 lineage in red and *Dmbx* expression in green. Dotted line represents the embryo midline. In second and third panels, both hemispheres are visible but only the left side has been electroporated. In *Coe>Vsx* condition, *Dmbx* expression is seen mainly in unelectroporated hemispheres, indicating that *Vsx* represses *Dmbx*. Left-right mosaic incorporation of plasmid thus provides us with an internal control. In *Coe>Islet, Dmbx* expression is just as likely to be seen in electroporated hemispheres as in unelectroporated hemispheres. This indicates relative lack of repression of *Dmbx* by Islet. Arrow indicates A12.239. (**B**) As in A, but instead looking at effects of Dmbx and Islet overexpression on *Vsx*. Open arrowhead indicates A13.474 cell; closed arrowhead indicates A11.117. Dmbx appears to repress *Vsx* in both cells, while Islet appears to repress *Vsx* in A11.117 but not in A13.474. Thus, although in our quantitative assay *Coe>Islet* is indistinguishable from the control, there is a qualitative difference between the two (A11.117-specific loss of *Vsx*). (**C**) Same as in A and B, but instead looking at effects of Dmbx and Vsx overexpression on *Islet (Isl)*. *Islet* is expressed in A10.57 (open arrows), therefore we scored for 'adjacent' *Fgf8/17/18>lacZ* and neuronal *Islet* expression, instead of colocalization. *Islet* expression is also seen in the notochord, just ventral to the nerve cord. This notochord expression was not assayed. Double arrowhead indicates ectopic *Islet* expression in A12.239 caused by overexpression of *Vsx*. All in situ hybridizations carried out on a mixture of embryos at stages 23-25, from at least three independent electroporations per condition. (**D**) Larva electroporated with *Coe>Dmbx* and *Fgf8/17/18>GFP*. Axons from A9.30 descendants in the VG project down the tail but do not form motor endplates (inset). (**E**) Larva electroporated with *Coe>Vsx* and *Fgf8/17/18>GFP*, showing lack of endplates as in D. (**F**) Larva electroporated with *Coe>Islet* and *Fgf8/17/18*, showing endplates typical of control larvae. (**G**) Same as in F, but in a larva electroporated with *Coe>Nk6* instead. (**H**) Quantification of endplate formation under conditions represented in D-G, plus *Coe>lacZ* control. Larvae were assayed for frondose endplates visible by GFP fluorescence, from *Fgf8/17/18>GFP* expression in A9.30 lineage. Bars represent percentage of larvae showing endplates, averaged over three replicates (±s.e.m.). Embryos in A-C were from a batch of mixed stages, from E65-E80.

autonomous effects of having multiple A11.117 cells in contact with each other, or could be related to lower levels of *Pitx* expression. However, the lack of endplates, the ipsilateral axon trajectory, and cell shape and size indicate an acquisition of the A11.117 fate. Thus, there is a correlation between transcriptional state (*Vsx*+, *Pitx*+) and neuronal morphology in the VG.

Conversion of visceral ganglion precursors into ectopic A12.239-like neurons

We next investigated whether other signaling pathways might be acting to specify the other neurons in the VG. We perturbed Notch signaling in the A9.30 lineage, using the *Fgf8/17/18* enhancer to express a mutant form of Su(H) incapable of binding DNA [Su(H)^{DBM}] (Hudson and Yasuo, 2006). Upon *Fgf8/17/18> Su(H)^{DBM}* electroporation, both A12.237 and A12.239 (the posterior daughter cells of A11.119 and A11.120, respectively) express Dmbx. As a result, a striking 'off-on-off-on' GFP pattern is seen in 66% (n=100) of embryos electroporated with *Fgf8/17/18> Su(H)^{DBM}* and *Dmbx>GFP* (Fig. 7E). An alternating pattern of endogenous *Dmbx* expression is also seen by in situ hybridization (Fig. 7F). In 100% (n=100) of wild-type embryos, A12.239 is the only cell that expresses *Dmbx* (Fig. 7D). This 'off-on-off-on' phenotype suggests the specification of an ectopic A12.239-like neuron is not due to a simple breakdown in lateral

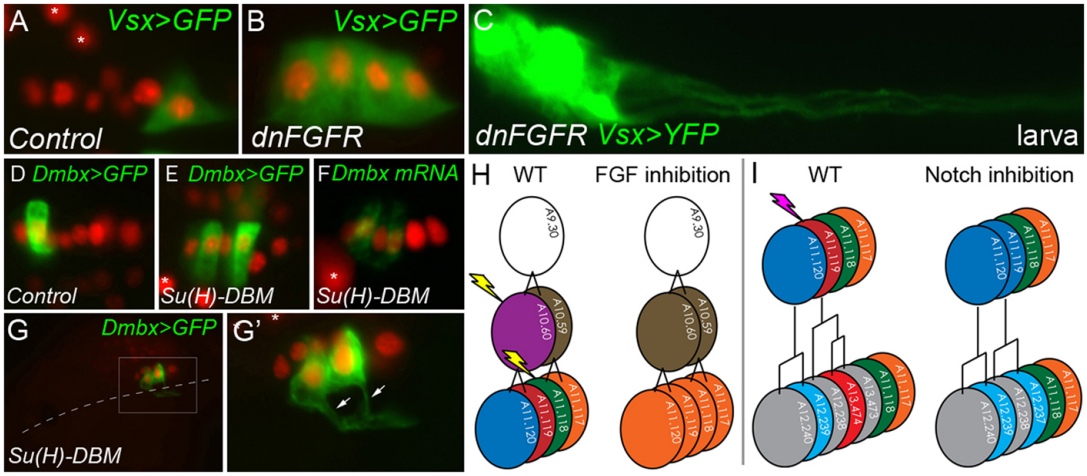

Fig. 7. Inhibition of FGF and Notch signaling pathways alters the specification of VG neural precursors. (**A**) At stage E75 (15.5 hpf), *Vsx>GFP* (green) is normally visible only in A11.117. (**B**) A9.30 descendants at stage E75 uniformly expressing *Vsx>GFP* upon perturbation of FGF signaling by *Fgf8/17/18>dnFgfr*. (**C**) Ectopic *Vsx+* neurons in a swimming tadpole electroporated with *Fgf8/17/18>dnFgfr.* (**D**) Control (co-electroporated with *Dmbx>GFP* and *Fgf8/17/18>lacZ)* embryo showing *Dmbx>GFP* expression (green) in A12.239 at stage E75. (**E**) Upon inhibition of Notch signaling by co-electroporation with *Fgf8/17/18>Su(H)DBM*, *Dmbx>GFP* is seen to be expressed in two A9.30 descendants, instead of just one (same stage as in D, see text for details). (**F**) Ectopic *Dmbx* expression confirmed by in situ hybridization (green) at stage E65 (14.5 hpf). (**G**) Dorsal view of a stage E90 (17.5 hpf) embryo electroporated with *Fgf8/17/18>Su(H)DBM* and *Dmbx>GFP* (green). Embryonic midline marked by broken line. (**G′**) Magnified view of inset in G, showing both *Dmbx+* cells growing axons, both of which are crossing the midline (arrows). A9.30 lineage in A,B and D-G′ is labeled with *Fgf8/17/18>Histone2B::mCherry* or *lacZ* (red). Asterisks in A,E,F,G′ denote mesenchyme cells expressing *Fgf8/17/18.* (**H**) The mitotic history of the A9.30 lineage from stages E50 to E80 (from top to bottom), indicating putative FGF signaling events (yellow thunderbolts) distinguishing A10.60 from A10.59 and A11.118 from A11.117 in wild-type embryos (left). Inhibiting FGF signaling (right) transforms the entire lineage to an A11.117-like fate (orange), as seen in B. (**I**) A9.30 mitotic history from E55 to E80. Pink thunderbolt indicates putative Notch signaling event required for specification of A11.119. Upon inhibition of Notch, A11.119 adopts a A11.120 fate, giving rise to an ectopic A12.239-like descendant (light blue) as seen in F,G.

inhibition of neurogenesis. Rather, it suggests a conversion of A11.119 into an A11.120-like progenitor cell upon inhibition of Notch signaling (summarized in Fig. 7I). By contrast, perturbation of Notch signaling in the A9.30 lineage does not affect the specification of A11.117 and A11.118, based on the lack of ectopic *Dmbx>GFP* expression in these cells, and normal *Vsx>GFP* expression in A11.117 (see Fig. S6B in the supplementary material)

Moreover, in 25% (n=300) of *Fgf8/17/18>Su(H)*^{DBM}-electroporated embryos, ectopic *Dmbx+* neurons grew axons that crossed the midline (Fig. 7G; see Fig. S6A in the supplementary material). Thus, ectopic *Dmbx+* neurons project contralaterally, a feature unique to the *Dmbx+* A12.239 pair within the VG. This observation suggests that the contralateral projection of A12.239 correlates with a unique transcriptional state as assayed by *Dmbx* expression; duplicating a transcriptional state results in a duplicate neuron with the same axon trajectory.

DISCUSSION

We have used enhancers associated with TFs expressed in specific VG neuronal precursors to visualize the neurons controlling the swimming behavior of the *Ciona* tadpole. We have shown that neuronal subtypes in the *Ciona* VG arise in a stereotyped manner from cells expressing distinct combinations of TFs, which correlate with specific morphological features such as contralaterally projecting axons and frondose motor endplates (summarized in Fig. 5). These qualitative traits were largely invariant, though gross errors in axon outgrowth and targeting were sporadically seen in embryos displaying other non-specific developmental defects attributed to the electroporation protocol. Our observations on cell-specific morphological attributes such as cell shape and axon trajectory are consistent with previous studies that distinguished each neuron based on their position within the VG (Imai and Meinertzhagen, 2007; Takamura et al., 2010).

These neuron-specific reporter constructs should be useful for the visualization and manipulation of individual neurons in vivo. In fact, with a combination of three enhancers and three different fluorescent reporter genes, we were able to distinguish five pairs of neurons in a single tadpole through co-electroporation and multi-plexed fluorescent imaging (Fig. 5). This *Ciona* ‘brainbow’ (Livet et al., 2007) demonstrates the potential usefulness of these constructs as a tool for future studies on the ascidian CNS.

We have begun to document the exact signaling events involved in setting up the transcriptional and subsequent morphological diversity of the ascidian VG. These signaling events are not necessarily shared with vertebrates. For example, the *Ciona* neural tube is comprised of cells arranged in just four rows: one ventral, one dorsal and two lateral rows. All VG neurons arise from cells within the lateral rows. It is hard to reconcile this simple layout with dorsoventral patterning by long-range BMP and Shh signals in the vertebrate neural tube (Dessaud et al., 2008). The short-range patterning of the *Ciona* neural tube might instead depend on ascidian-specific processes. We have already shown that FGF and Notch are two signaling pathways involved in VG neuronal subtype specification. Signaling events used for a given cell fate decision can vary even between different ascidian species (Hudson and Yasuo, 2008), indicating flexibility of signaling pathway deployment in evolution. However, we believe the transcriptional networks operating downstream of cell fate choice may prove to be more conserved, and thus more interesting from a comparative standpoint.

It has been assumed that all five pairs of neurons in the VG are motoneurons, based on their expression of cholinergic markers (Horie et al., 2010). However, only A11.118 forms the large lateral motor endplates, whereas A10.57 forms smaller endplates. In vertebrates and *Drosophila*, motoneurons and interneurons are specified by a 'motoneuron code'. The combinatorial activity of Islet and Lhx3 specifies primary motoneurons, while interneurons are specified in the absence of Islet, through action of Chx10/Vsx2 (Lee et al., 2008; Thaler et al., 2002; Thor et al., 1999). Our study suggests this regulatory code might also apply to the VG of *Ciona*. For example, *Islet* and *Lhx3* are transiently co-expressed in A10.57, A11.117 and A11.118 (Katsuyama et al., 2005; Imai et al., 2009). The putative interneuron A11.117 goes on to express *Vsx,* consistent with conservation of a motoneuron code. The inhibition of motor endplate formation by misexpression of Vsx can be interpreted as the specification of ectopic interneurons at the expense of motoneurons.

We have also found a correlation between *Dmbx* expression and contralateral projections in the VG. Ectopic *Dmbx*+ neurons project contralaterally. In mice, *Dmbx1* is expressed initially in the prospective midbrain, and later in hindbrain and spinal cord neurons (Gogoi et al., 2002). *Dmbx1* knockout mice show early neonatal lethality owing to diminished milk intake, probably related to its function in the hindbrain (Fujimoto et al., 2007; Ohtoshi and Behringer, 2004). In zebrafish, *Dmbx1* paralogs in zebrafish have been shown to regulate cell-cycle exit of neuronal progenitors in the retina and optic tectum (Kawahara et al., 2002; Wong et al., 2010). It is possible that Dmbx genes are involved in a regulatory code for decussating interneuron subtypes in vertebrates, such as the aforementioned Mauthner cells of fish and amphibians.

Future work will be required to determine the causal link between TFs and morphology in the VG. A gene network analysis might reveal the regulation of rate-limiting cellular effectors responsible for some of the distinctive properties of VG neurons. It is also possible that some TFs might regulate transient cellular processes, such as morphogenetic movements, rather than subtype identity. However, some possibly represent 'selector genes' that directly regulate the terminal differentiation genes responsible for subtype-specific morphological and physiological properties (Hobert et al., 2010). Future work on how these distinct neurons interconnect to control swimming will bring us closer to understanding how gene regulatory networks create behavior in a chordate.

Acknowledgements

We thank Justin Bosch, Phillip Cleves and Andy Cooc for assistance; the members of the Levine Lab for insightful discussion and suggestions; and Lionel Christiaen for critical reading of the manuscript. Supported by NSF grant IOB 0445470 to M.L. and an ARCS fellowship to A.S.

Competing interests statement

The authors declare no competing financial interests.

Supplementary material

Supplementary material for this article is available at
http://dev.biologists.org/lookup/suppl/doi:10.1242/dev.061507/-/DC1

References

Beh, J., Shi, W., Levine, M., Davidson, B. and Christiaen, L. (2007). FoxF is essential for FGF-induced migration of heart progenitor cells in the ascidian Ciona intestinalis. *Development* **134**, 3297-3305.

Bertrand, V., Hudson, C., Caillol, D., Popovici, C. and Lemaire, P. (2003). Neural tissue in ascidian embryos is induced by FGF9/16/20, acting via a combination of maternal GATA and Ets transcription factors. *Cell* **115**, 615-627.

Brown, E. R., Nishino, A., Bone, Q., Meinertzhagen, I. A. and Okamura, Y. (2005). GABAergic synaptic transmission modulates swimming in the ascidian larva. *Eur. J. Neurosci.* **22**, 2541-2548.

Chabry, L. (1887). *Embryologie Normale et Tératologique des Ascidies*: F. Alcan.

Christiaen, L., Bourrat, F. and Joly, J. (2005). A modular cis-regulatory system controls isoform-specific pitx expression in ascidian stomodeum. *Dev. Biol.* **277**, 557-566.

Christiaen, L., Wagner, E., Shi, W. and Levine, M. (2009). The sea squirt ciona intestinalis. *Cold Spring Harbor Protoc.* **2009**, pdb.emo138.

Cole, A. G. and Meinertzhagen, I. A. (2001). Tailbud embryogenesis and the development of the neurohypophysis in the ascidian Ciona intestinalis. In *The Biology of Ascidians* (ed. H., Sawada, H., Yokosawa and C. C. Lambert), pp. 137-141. Tokyo: Springer-Verlag.

Cole, A. G. and Meinertzhagen, I. A. (2004). The central nervous system of the ascidian larva: mitotic history of cells forming the neural tube in late embryonic Ciona intestinalis. *Dev. Biol.* **271**, 239-262.

Conklin, E. G. (1905). Mosaic development in ascidian eggs. *J. Exp. Zool.* **2**, 145-223.

Corbo, J., Levine, M. and Zeller, R. (1997). Characterization of a notochord-specific enhancer from the Brachyury promoter region of the ascidian, Ciona intestinalis. *Development* **124**, 589-602.

Davidson, B., Shi, W., Beh, J., Christiaen, L. and Levine, M. (2006). FGF signaling delineates the cardiac progenitor field in the simple chordate, *Ciona intestinalis*. *Genes Dev.* **20**, 2728-2738.

Dehal, P., Satou, Y., Campbell, R. K., Chapman, J., Degnan, B., De Tomaso, A., Davidson, B., Di Gregorio, A., Gelpke, M., Goodstein, D. M. et al. (2002). The draft genome of Ciona intestinalis: insights into chordate and vertebrate origins. *Science* **298**, 2157-2167.

Delsuc, F., Brinkmann, H., Chourrout, D. and Philippe, H. (2006). Tunicates and not cephalochordates are the closest living relatives of vertebrates. *Nature* **439**, 965-968.

Dessaud, E., McMahon, A. and Briscoe, J. (2008). Pattern formation in the vertebrate neural tube: a sonic hedgehog morphogen-regulated transcriptional network. *Development* **135**, 2489-2503.

Dilly, N. (1964). Studies on receptors in cerebral vesicle of ascidian tadpole.2. ocellus. *Q. J. Microsc. Sci.* **105**, 13-20.

Dilly, P. N. (1962). Studies on receptors in cerebral vesicle of ascidian tadpole.1. otolith. *Q. J. Microsc. Sci.* **103**, 393-397.

Dubois, L. and Vincent, A. (2001). The COE-Collier/Olf1/EBF-transcription factors: structural conservation and diversity of developmental functions. *Mech. Dev.* **108**, 3-12.

Dufour, H. D., Chettouh, Z., Deyts, C., de Rosa, R., Goridis, C., Joly, J. S. and Brunet, J. F. (2006). Precraniate origin of cranial motoneurons. *Proc. Natl. Acad. Sci. USA* **103**, 8727-8732.

Dynes, J. and Ngai, J. (1998). Pathfinding of olfactory neuron axons to stereotyped glomerular targets revealed by dynamic imaging in living zebrafish embryos. *Neuron* **20**, 1081-1091.

Eaton, R., Lee, R. and Foreman, M. (2001). The Mauthner cell and other identified neurons of the brainstem escape network of fish. *Prog. Neurobiol.* **63**, 467-485.

Edwards, K., Demsky, M., Montague, R., Weymouth, N. and Kiehart, D. (1997). GFP-Moesin illuminates actin cytoskeleton dynamics in living tissue and demonstrates cell shape changes during morphogenesis in *Drosophila*. *Dev. Biol.* **191**, 103-117.

Enjin, A., Rabe, N., Nakanishi, S., Vallstedt, A., Gezelius, H., Memic, F., Lind, M., Hjalt, T., Tourtellotte, W. and Bruder, C. (2010). Identification of novel spinal cholinergic genetic subtypes disclose Chodl and Pitx2 as markers for fast motor neurons and partition cells. *J. Comp. Neurol.* **518**, 2284-2304.

Fujimoto, W., Shiuchi, T., Miki, T., Minokoshi, Y., Takahashi, Y., Takeuchi, A., Kimura, K., Saito, M., Iwanaga, T. and Seino, S. (2007). Dmbx1 is essential in agouti-related protein action. *Proc. Natl. Acad. Sci. USA* **104**, 15514-15519.

Giuliano, P., Marino, R., Pinto, M. and De Santis, R. (1998). Identification and developmental expression of Ci-isl, a homologue of vertebrate islet genes, in the ascidian Ciona intestinalis. *Mech. Dev.* **78**, 199-202.

Gogoi, R., Schubert, F., Martinez-Barbera, J., Acampora, D., Simeone, A. and Lumsden, A. (2002). The paired-type homeobox gene Dmbx1 marks the midbrain and pretectum. *Mech. Dev.* **114**, 213-217.

Goulding, M. (2009). Circuits controlling vertebrate locomotion: moving in a new direction. *Nat. Rev. Neurosci.* **10**, 507-518.

Hobert, O., Carrera, I. and Stefanakis, N. (2010). The molecular and gene regulatory signature of a neuron. *Trends Neurosci.* **33**, 435-445.

Horie, T., Kusakabe, T. and Tsuda, M. (2008a). Glutamatergic networks in the Ciona intestinalis larva. *J. Comp. Neurol.* **508**, 249-263.

Horie, T., Sakurai, D., Ohtsuki, H., Terakita, A., Shichida, Y., Usukura, J., Kusakabe, T. and Tsuda, M. (2008b). Pigmented and nonpigmented ocelli in the brain vesicle of the ascidian larva. *J. Comp. Neurol.* **509**, 88-102.

Horie, T., Nakagawa, M., Sasakura, Y., Kusakabe, T. G. and Tsuda, M. (2010). Simple motor system of the ascidian larva: neuronal complex comprising putative cholinergic and GABAergic/glycinergic neurons. *Zool. Sci.* **27**, 181-190.

Hudson, C. and Yasuo, H. (2006). A signalling relay involving Nodal and Delta ligands acts during secondary notochord induction in Ciona embryos. *Development* **133**, 2855-2864.
Hudson, C. and Yasuo, H. (2008). Similarity and diversity in mechanisms of muscle fate induction between ascidian species. *Biol. Cell* **100**, 265-277.
Hudson, C., Lotito, S. and Yasuo, H. (2007). Sequential and combinatorial inputs from Nodal, Delta2/Notch and FGF/MEK/ERK signalling pathways establish a grid-like organisation of distinct cell identities in the ascidian neural plate. *Development* **134**, 3527-3537.
Ikuta, T. and Saiga, H. (2007). Dynamic change in the expression of developmental genes in the ascidian central nervous system: revisit to the tripartite model and the origin of the midbrain-hindbrain boundary region. *Dev. Biol.* **312**, 631-643.
Imai, J. and Meinertzhagen, I. (2007). Neurons of the ascidian larval nervous system in Ciona intestinalis: I. Central nervous system. *J. Comp. Neurol.* **501**, 316-334.
Imai, K., Levine, M., Satoh, N. and Satou, Y. (2006). Regulatory blueprint for a chordate embryo. *Science* **312**, 1183-1187.
Imai, K., Stolfi, A., Levine, M. and Satou, Y. (2009). Gene regulatory networks underlying the compartmentalization of the Ciona central nervous system. *Development* **136**, 285-293.
Jiang, D., Tresser, J., Horie, T., Tsuda, M. and Smith, W. (2005). Pigmentation in the sensory organs of the ascidian larva is essential for normal behavior. *J. Exp. Biol.* **208**, 433-438.
Kajiwara, S. and Yoshida, M. (1985). Changes in behavior and ocellar structure during the larval life of solitary ascidians. *Biol. Bull.* **169**, 565-577.
Katsuyama, Y., Okada, T., Matsumoto, J., Ohtsuka, Y., Terashima, T. and Okamura, Y. (2005). Early specification of ascidian larval motor neurons. *Dev. Biol.* **278**, 310-322.
Kawahara, A., Chien, C. and Dawid, I. (2002). The homeobox gene mbx is involved in eye and tectum development. *Dev. Biol.* **248**, 107-117.
Kimura, Y., Okamura, Y. and Higashijima, S. (2006). *alx*, a zebrafish homolog of *Chx10*, marks ipsilateral descending excitatory interneurons that participate in the regulation of spinal locomotor circuits. *J. Neurosci.* **26**, 5684-5697.
Lee, S., Lee, B., Joshi, K., Pfaff, S., Lee, J. and Lee, S. (2008). A regulatory network to segregate the identity of neuronal subtypes. *Dev. Cell* **14**, 877-889.
Livet, J., Weissman, T., Kang, H., Lu, J., Bennis, R., Sanes, J. and Lichtman, J. (2007). Transgenic strategies for combinatorial expression of fluorescent proteins in the nervous system. *Nature* **450**, 56-62.
Mackie, G. and Bone, Q. (1976). Skin impulses and locomotion in an ascidian tadpole. *J. Mar. Biolog. Assoc. UK* **56**, 751-768.
Meinertzhagen, I., Lemaire, P. and Okamura, Y. (2004). The neurobiology of the ascidian tadpole larva: recent developments in an ancient chordate. *Neuroscience* **27**, 453-485.
Meinertzhagen, I. A. and Okamura, Y. (2001). The larval ascidian nervous system: the chordate brain from its small beginnings. *Trends Neurosci.* **24**, 401-410.
Nagatomo, K. and Fujiwara, S. (2003). Expression of Raldh2, Cyp26 and Hox-1 in normal and retinoic acid-treated Ciona intestinalis embryos. *Gene Expr. Patterns* **3**, 273-277.
Nicol, D. and Meinertzhagen, I. A. (1988). Development of the central nervous system of the larva of the ascidian, Ciona intestinalis L. I. The early lineages of the neural plate. *Dev. Biol.* **130**, 721-736.
Nicol, D. and Meinertzhagen, I. A. (1991). Cell counts and maps in the larval central nervous system of the ascidian Ciona intestinalis (L.). *J. Comp. Neurol.* **309**, 415-429.
Ohmori, H. and Sasaki, S. (1977). Development of neuromuscular transmission in a larval tunicate. *J. Physiol.* **269**, 221-254.
Ohtoshi, A. and Behringer, R. (2004). Neonatal lethality, dwarfism, and abnormal brain development in *Dmbx1* mutant mice. *Mol. Cell. Biol.* **24**, 7548-7558.
Okada, T., MacIsaac, S., Katsuyama, Y., Okamura, Y. and Meinertzhagen, I. (2001). Neuronal form in the central nervous system of the tadpole larva of the ascidian *Ciona intestinalis*. *Biol. Bull.* **200**, 252-256.
Okada, T., Katsuyama, Y., Ono, F. and Okamura, Y. (2002). The development of three identified motor neurons in the larva of an ascidian, Halocynthia roretzi. *Dev. Biol.* **244**, 278-292.
Rothbächer, U., Bertrand, V., Lamy, C. and Lemaire, P. (2007). A combinatorial code of maternal GATA, Ets and -catenin-TCF transcription factors specifies and patterns the early ascidian ectoderm. *Development* **134**, 4023-4032.
Sato, S. and Yamamoto, H. (2001). Development of pigment cells in the brain of ascidian tadpole larvae: insights into the origins of vertebrate pigment cells. *Pigment Cell Res.* **14**, 428-436.
Satoh, N. (2003). Ciona intestinalis: an emerging model for whole-genome analyses. *Trends Genet.* **19**, 376-381.
Stolfi, A., Gainous, T., Young, J., Mori, A., Levine, M. and Christiaen, L. (2010). Early chordate origins of the vertebrate second heart field. *Science* **329**, 565-568.
Svendsen, P. and McGhee, J. (1995). The C. elegans neuronally expressed homeobox gene ceh-10 is closely related to genes expressed in the vertebrate eye. *Development* **121**, 1253-1262.
Takahashi, T. and Holland, P. (2004). Amphioxus and ascidian Dmbx homeobox genes give clues to the vertebrate origins of midbrain development. *Development* **131**, 3285-3294.
Takamura, K. (1998). Nervous network in larvae of the ascidian Ciona intestinalis. *Dev. Genes Evol.* **208**, 1-8.
Takamura, K., Egawa, T., Ohnishi, S., Okada, T. and Fukuoka, T. (2002). Developmental expression of ascidian neurotransmitter synthesis genes. *Dev. Genes Evol.* **212**, 50-53.
Takamura, K., Minamida, N. and Okabe, S. (2010). Neural map of the larval central nervous system in the Ascidian Ciona intestinalis. *Zool. Sci.* **27**, 191-203.
Thaler, J., Lee, S., Jurata, L., Gill, G. and Pfaff, S. (2002). LIM factor Lhx3 contributes to the specification of motor neuron and interneuron identity through cell-type-specific protein-protein interactions. *Cell* **110**, 237-249.
Thor, S., Andersson, S., Tomlinson, A. and Thomas, J. (1999). A LIM-homeodomain combinatorial code for motor-neuron pathway selection. *Nature* **397**, 76-80.
Tsuda, M., Sakurai, D. and Goda, M. (2003). Direct evidence for the role of pigment cells in the brain of ascidian larvae by laser ablation. *J. Exp. Biol.* **206**, 1409-1417.
Wada, H., Holland, P., Sato, S., Yamamoto, H. and Satoh, N. (1997). Neural tube is partially dorsalized by overexpression ofhrpax-37: the ascidian homologue ofPax-3andPax-7. *Dev. Biol.* **187**, 240-252.
Wong, L., Weadick, C., Kuo, C., Chang, B. and Tropepe, V. (2010). Duplicate *dmbx1* genes regulate progenitor cell cycle and differentiation during zebrafish midbrain and retinal development. *BMC Dev. Biol.* **10**, 100.
Yoshida, R., Sakurai, D., Horie, T., Kawakami, I., Tsuda, M. and Kusakabe, T. (2004). Identification of neuron-specific promoters in Ciona intestinalis. G*enesis* **39**, 130-140.